Research Article

Zhihong Zhang, Zhenxiu Shan, Rubin Chen, Xiaorong Peng, Bin Xu, Liang Xiao, Guofei Zhang*

circ_0005962 functions as an oncogene to aggravate NSCLC progression

https://doi.org/10.1515/med-2021-0255
received July 30, 2020; accepted February 26, 2021

Abstract

Background – Non-small cell lung cancer (NSCLC) is a leading threat to human lives with high incidence and mortality. Circular RNAs were reported to play important roles in human cancers. The purpose of this study was to investigate the role of circ_0005962 and explore the underlying functional mechanisms.

Methods – The protein levels of Beclin 1, light chain3 (LC3-II/LC3-I), Pyruvate dehydrogenase kinase 4 (PDK4), Cleaved Caspase 3 (C-caspase 3), and proliferating cell nuclear antigen were examined using western blot analysis. Glycolysis was determined according to the levels of glucose consumption and lactate production. Xenograft model was constructed to investigate the role of circ_0005962 *in vivo*.

Result – circ_0005962 expressed with a high level in NSCLC tissues and cells. circ_0005962 knockdown inhibited proliferation, autophagy, and glycolysis but promoted apoptosis in NSCLC cells. miR-382-5p was targeted by circ_0005962, and its inhibition reversed the role of circ_0005962 knockdown. Besides, PDK4, a target of miR-382-5p, was regulated by circ_0005962 through miR-382-5p, and its overexpression abolished the effects of miR-382-5p reintroduction. circ_0005962 knockdown suppressed tumor growth *in vivo*.

Conclusion – circ_0005962 knockdown restrained cell proliferation, autophagy, and glycolysis but stimulated apoptosis through modulating the circ_0005962/miR-382-5p/PDK4 axis. Our study broadened the insights into understanding the mechanism of NSCLC progression.

Keywords: circ_0005962, miR-382-5p, PDK4, NSCLC

1 Introduction

Lung cancer is a leading cause of cancer-related death worldwide [1]. Lung cancer is the second most common cancer among men and women: second only to prostate cancer in men, and second only to breast cancer in women [2]. Non-small cell lung cancer (NSCLC) and small cell lung cancer are two types of lung cancer, and NSCLC accounts for about 85% of all lung cancer cases [3]. NSCLC, including large cell carcinoma, squamous cell carcinoma, and adenocarcinoma, is associated with high incidence and mortality [4,5]. Clinically, treatment modalities, including chemotherapy and surgery, are used to treat NSCLC, but the 5-year overall survival rate for all stages of NSCLC patients is only 16% [2,6]. The severe situation of NSCLC treatment makes it urgent to further explore the mechanism of occurrence and development of NSCLC to establish novel therapeutic strategies.

Circular RNAs (circRNAs) belong to non-coding RNAs and derive from precursor mRNAs by "back-splicing." circRNAs are mostly detected in the cytoplasm and function as competing endogenous RNAs (ceRNAs) to work as microRNA (miRNA) sponges [7–9]. Advances of high-throughput RNA sequencing in the identification of circRNAs hinted that circRNAs participated in the pathogenesis of cancers [10]. Recent studies stated that circRNAs played vital roles in the development of NSCLC. For example, circ_100146 functioned as an oncogene, and its suppression hindered cell proliferation and invasion [11]. circP4HB overexpression promoted epithelial–mesenchymal transition (EMT), thus inducing metastatic ability in NSCLC [12]. circRNA F-circEA-2a contributed to cell migration and invasion but had little role in cell

* **Corresponding author: Guofei Zhang,** Department of Gastrointestinal Surgery, Gong'an County People's Hospital, No. 119, Chan Ling Road, Douhudi Town, Gong'an County, Jingzhou, Hubei 433000, China, e-mail: hwzvkl@163.com, tel: +86-716-5234334
Zhihong Zhang, Zhenxiu Shan: Department of Oncology, Gong'an County People's Hospital, Hubei 433000, China
Rubin Chen: Department of Radiology, Gong'an County People's Hospital, Hubei 433000, China
Xiaorong Peng: Department of Pathology, Gong'an County People's Hospital, Hubei 433000, China
Bin Xu: Department of Oncology, Renmin Hospital of Wuhan University, Hubei General Hospital, Hubei 433000, China
Liang Xiao: Department of Cerebral Surgery, Gong'an County People's Hospital, Hubei 433000, China

proliferation [13]. A former study obtained dozens of circRNAs through the circBase database and CSCD database for comparison between lung adenocarcinoma tissues and paired non-tumor tissues [14], and circ_0005962, back-spliced from tyrosine 3-monooxygenase/tryptophan 5-monooxygenase activation protein zeta (YWHAZ), was one of the significantly upregulated circRNAs and had valuable prognostic significance. However, the understanding of the specific roles of circ_0005962 in NSCLC remained lacking and requires further exploration.

miRNAs are known as small non-coding RNAs with 18–23 nucleotides [15]. It is well documented that circRNAs played functions by acting as miRNA sponges [9]. Interestingly, bioinformatics analysis found that miR-382-5p was a potential target of circ_0005962. miR-382-5p was frequently mentioned in different cancers, including glioma, oral squamous cell carcinoma, and breast cancer [16–18]. Unfortunately, the role of miR-382-5p in NSCLC was largely unknown, and the interactions between circ_0005962 and miR-382-5p had not been declared.

One of the important functions of pyruvate dehydrogenase kinase (PDK) is to regulate the metabolic conversion from mitochondrial respiration to cytoplasmic glycolysis [19]. Glycolysis is a preferential way for tumor cells to obtain energy [20]. Pyruvate dehydrogenase kinase 4 (PDK4), one of the PDK family protein kinases, is located on chromosome 7q21.3 [21]. PDK4 was reported to be implicated in numerous cellular activities, such as cell proliferation, metastasis, drug resistance, glycolysis, and autophagy in different types of cancers [21–23]. Intriguingly, bioinformatics analysis discovered that PDK4 was a putative target of miR-382-5p, which was further clarified in NSCLC development in our study.

In the present study, we measured the expression of circ_0005962 in NSCLC tissues and cells. Functional analyses revealed the role of circ_0005962 in cell proliferation, autophagy, glycolysis, and apoptosis. Besides, we constructed circRNA–miRNA–mRNA regulatory axis to expound the potential mechanism of circ_0005962 in NSCLC. Our study aimed to provide new sights for the understanding of NSCLC development and supply promising biomarkers.

2 Materials and methods

2.1 Tissues and cell lines

A total of 45 tumor tissues and adjacent normal tissues from NSCLC patients were collected from Gong'an County People's Hospital. Informed consent was signed by each subject. All tissues were immediately placed into liquid nitrogen and stored at −80°C ultra low-temperature refrigerator. This research obtained the approval of the Ethics Committee of Gong'an County People's Hospital.

NSCLC cell lines (A549 and HCC827) and human bronchial epithelial cells (BEAS-2B) were purchased from Zishi Biotechnology (Shanghai, China). A549 and HCC827 cells were maintained in 90% Roswell Park Memorial Institute 1640 (RPMI 1640; Sigma, St. Louis, MO, USA) containing 10% fetal bovine serum (FBS; Sigma). BEAS-2B cells were cultured in 90% Dulbecco's Modified Eagle Medium (DMEM; Sigma) containing 10% FBS (Sigma). All mediums were placed at 37°C containing 5% CO_2.

2.2 Quantitative real-time polymerase chain reaction (qPCR)

Trizol reagent (Beyotime, Shanghai, China) was utilized to isolate total RNA from tissues and cells. The complementary DNA (cDNA) was assembled using the riboSCRIPT Reverse Transcription Kit (Ribobio, Guangzhou, China). Then the amplification reaction was carried out using SYBR Green Master PCR mix (Beyotime) through the ABI 7900 system (Applied Biosystems, Foster City, CA, USA). The relative expression was normalized using glyceraldehyde-3-phosphate dehydrogenase (GAPDH) or small nuclear RNA U6 and calculated using $2^{-\Delta\Delta Ct}$ method. The primers used were listed as below:

circ_0005962, F: 5′-AACTCCCCAGAGAAAGCCTGC-3′ and R: 5′-TGCTTGTGAAGCATTGGGGAT-3′; YWHAZ, F: 5′-ACTTTTGGTACATTGTGGCTTCAA-3′ and R: 5′-CCGCCAGGACAAACCAGTAT-3′; PDK4, F: 5′-GGAGCATTTCTCGCGCTACA-3′ and R: 5′-ACAGGCAATTCTTGTCGCAAA-3′; GAPDH, F: 5′-CTGGGCTACACTGAGCACC-3′ and R: 5′-AAGTGGTCGTTGAGGGCAATG-3′; miR-382-5p, F: 5′-ATCCGTGAAGTTGTTCGTGG-3′ and R: 5′-TATGGTTGTAGAGGACTCCTTGAC-3′; U6, F: 5′-CTCGCTTCGGCAGCACATATACT-3′ and R: 5′-ACGCTTCACGAATTTGCGTGTC-3′.

2.3 Chromogenic *in situ* hybridization (CISH) assay

Digoxigenin (DIG)-labeled circ_0005962 probe at the 5′ and 3′ ends was synthesized by Sangon Biotech (Shanghai, China). Tissue microarray which contained 45 cases with paired tumor tissues and non-tumor tissues was used to perform CISH analysis. In brief, paraffin tissue slides were

incubated with proteinase K (20 μg/mL; Servicebio, Wuhan, China; 37°C, 30 min). The slides were then used for prehybridization in a hybridization solution (Servicebio) at 37°C for 1 h, followed by incubation with fresh hybridization solution containing 500 nM of the corresponding probe at 4°C overnight. Slides were washed and blocked in serum-containing BSA for 30 min. The immunological reaction was carried out using anti-DIG-AP antibody (Roche, Basel, Switzerland) according to the manufacturer's protocol. The expression of circ_0005962 was detected by the BCIP/NBT substrates (Boster, Wuhan, China), and the stained specimens were observed using a bright field microscopy.

2.4 RNase R treatment

To confirm the stability and tolerance of circ_0005962, the RNA extraction was probed with or without RNase R (Applied Biological Materials Inc., Vancouver, Canada) at 37°C for 10 min. Then, the qPCR analysis was conducted as described above.

2.5 Cell transfection

Small interference RNA against circ_0005962 and negative control were synthesized by Sangon Biotech (Shanghai, China). The mimics of miR-382-5p (miR-382-5p), the inhibitor of miR-382-5p (anti-miR-382-5p), and respective negative control (NC or anti-NC) were purchased from Ribobio (Shanghai, China). The overexpression of circ_0005962 (circ_0005962) was performed as the previous study described [24] and constructed by Genechem (Shanghai, China), while the specific plasmid without the circ_0005962 cDNA was served as a control (circ-NC). The vector pcDNA3.1-PDK4 for the overexpression of PDK4 and the control pcDNA empty vector (vector) were constructed by Sangon Biotech. Lentiviral vector (Lenti-short hairpin) for stable NEAT1 downregulation (Lv-sh-circ_0005962) and the corresponding negative control (Lv-sh-NC) were obtained from Genechem. Cell transfection was conducted using Lipofectamine 3000 (Invitrogen, Carlsbad, CA, USA). Transfection efficiency and the following experiments were implemented after 48 h of transfection.

2.6 Cell counting kit-8 (CCK-8) assay

Cell proliferation was investigated using CCK-8 assay. A549 or HCC827 cells with different transfection were seeded into 96-well plates (5×10^3 cells/well). Then, cells interacted with CCK-8 solution (Beyotime) continuously for 2 h at 24, 48, and 72 h. The absorbance at 450 nm was measured using a microplate reader (Bio-Rad, Hercules, CA, USA).

2.7 Flow cytometry assay

Flow cytometry was applied to monitor cell apoptosis. After 48 h, A549 or HCC827 cells with different transfection were washed with phosphate buffer saline (PBS), probed with 0.25% trypsin, and resuspended in binding buffer. Afterward, the Annexin V-fluorescein isothiocyanate/propidium iodide apoptosis detection kit (Sigma) was used to doubly stain cells for 15 min in the dark. Eventually, the apoptotic cells were sorted using CellQuest software under a flow cytometer (Becton Dickinson, Franklin Lakes, NJ, USA).

2.8 Western blot

The western blot analysis was performed in line with a previous study described [25]. In brief, total proteins were separated and transferred into polyvinylidene fluoride (PVDF) membranes (Bio-Rad). After the block, the membranes were incubated with the primary antibodies and the secondary antibodies. Finally, the seeking proteins were visualized using the enhanced chemiluminescent reagent (Beyotime) through an imaging system (Bio-Rad). The antibodies used were listed as follows: anti-Beclin 1 (1:1,000; cat. no. ab210498; Abcam, Cambridge, MA, USA), anti-light chain3 (LC3) (1:2,000; cat. no. ab192890), anti-PDK4 (1:1,000; cat. no. ab89295), anti-Cleaved Caspase 3 (C-caspase 3) (1:1,000; cat. no. ab2302), anti- proliferating cell nuclear antigen (PCNA) (1:1,000; cat. no. ab92552), anti-GAPDH (1:1,000; cat. no. ab8245), and the horseradish peroxidase-conjugated secondary antibodies (1:5,000; cat. no. ab205718).

2.9 Detection of glucose consumption and lactate production

A549 or HCC827 cells with different transfection were planted into 96-well plates. After 48 h, cells were collected, washed three times with PBS, and then used for the detection of glucose consumption and lactate production using the Glucose Uptake Colorimetric Assay Kit and Lactate Assay Kit (Sigma) in agreement with the manufacturer's instructions.

2.10 Bioinformatics analysis

The targets of circRNA and miRNA were forecasted, and their binding sites were analyzed by the online bioinformatics tool circInteractome (https://circinteractome.nia.nih.gov/) and starbase (http://starbase.sysu.edu.cn/).

2.11 Dual-luciferase reporter assay

The dual-luciferase reporter assay was carried out for the verification of the relationship between miR-382-5p and circ_0005962 or PDK4. The partial frame of circ_0005962 containing the binding site or mutant binding site (wild-type or mutant-type) with miR-382-5p was amplified and cloned into the downstream of pGL4 vector (Promega, Madison, WI, USA) to generate circ_0005962-wt and circ_0005962-mut fusion plasmids. Likewise, the 3′UTR sequences of PDK4 harboring the binding site with miR-382-5p or mutant binding site (wild-type or mutant-type) were also amplified and inserted into the downstream of pGL4 vector to generate PDK4-wt and PDK-mut fusion plasmids. Subsequently, these fusion plasmids and miR-382-5p or NC were co-transfected into A549 and HCC827 cells, respectively. After 48 h, the cells were collected and detected using the Dual-luciferase assay system (Promega). The firefly luciferase activity was normalized by Renilla luciferase activity.

2.12 RNA immunoprecipitation (RIP) assay

RIP assay was executed to further confirm the relationship between miR-382-5p and circ_0005962 or PDK4. In one case, A549 and HCC827 cells were harvested and incubated with RNA lysis buffer. Then, cell lysate was incubated with RIP binding buffer containing magnetic beads coated with human Ago2 antibody or mouse IgG antibody (control) (Millipore, Billerica, MA, USA). Subsequently, the levels of circ_0005962 and miR-382-5p enriched in the beads were detected by qPCR. In another case, A549 and HCC827 cells transfected with miR-382-5p were lysed in RIP buffer with anti-Ago2- or IgG-bound magnetic beads. Next, the mRNA level of PDK4 enriched in the beads was examined by qPCR.

2.13 *In vivo* experiment

The mice experiment was approved by the Animal Care and Use Committee of Gong'an County People's Hospital. A total of 10 BALB/c nude mice (5-week-old, male) were purchased from HFK Bioscience (Beijing, China). A549 cells with Lv-sh-circ_0005962 or Lv-sh-NC transfection were subcutaneously injected into the back right flank of nude mice, dividing into the Lv-sh-circ_0005962 and Lv-sh-NC groups. Tumor volume was observed and recorded once a week following the algorithm (length × width^2 × 0.5), lasting 5 weeks. In the end, the mice were killed, and tumor samples were removed for weighting and further molecular studies.

2.14 Data analysis

The data were obtained from at least three times independent experimental analyses and conducted using SPSS 18.0 software (SPSS, Inc., Chicago, IL, USA). The survival curve was depicted via the Kaplan–Meier method. The correlation analysis was performed based on Spearman's correlation coefficient. Differences between the two groups were analyzed by Student's *t*-test or one-way analysis of variance among multiple groups. The data after processing were presented as the mean ± standard deviation, and $P < 0.05$ was considered to be statistically significant.

3 Result

3.1 High expression of circ_0005962 was observed in NSCLC tissues and cells and predicted the low survival rate of NSCLC patients

The expression of circ_0005962 was detected in NSCLC tissues and cell lines to observe whether circ_0005962 was aberrantly regulated in NSCLC. As shown in Figure 1a, the expression of circ_0005962 was significantly higher in tumor tissues (n = 45) than that in adjacent normal tissues (n = 45), and the data of circ_0005962 expression from CISH analysis was consistent with the data from qPCR. Besides, the expression of circ_0005962 was abundant in A549 and HCC827 cells relative to BEAS-2B cells (Figure 1b). Moreover, the survival curve was depicted utilizing Kaplan–Meier survival rate analysis according to the living status of NSCLC patients, and we found that the survival rate of patients with high expression of circ_0005962 was notably weaker compared with patients with low circ_0005962 expression (Figure 1c).

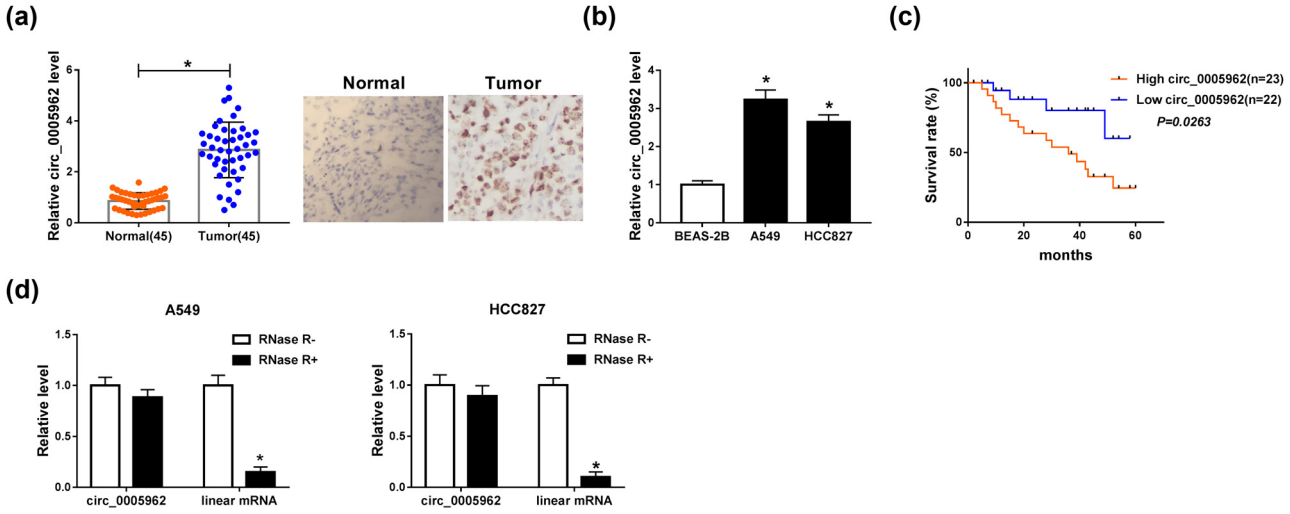

Figure 1: circ_0005962 was highly expressed in NSCLC tissues and cells. (a) The expression of circ_0005962 in tumor tissues (n = 45) and adjacent normal tissues (n = 45) was detected by qPCR. (b) The expression of circ_0005962 in NSCLC cell lines (A549 and HCC827) and normal cells (BEAS-2B) was detected by qPCR. (c) The survival curve was depicted according to the Kaplan–Meier plot and analyzed by the log-rank test. (d) The tolerance of circ_0005962 and corresponding linear RNA to RNase was measured according to their mRNA levels. *P < 0.05.

Additionally, the result of qPCR showed that the expression of circ_0005962 decreased a little with the treatment of RNase R, while the expression of the parental linear mRNA (YWHAZ) was significantly reduced with the treatment of RNase R, indicating that circ_0005962 was resistant to RNase R (Figure 1d). The data indicated that circ_0005962 was aberrantly upregulated in NSCLC.

3.2 circ_0005962 knockdown inhibited proliferation, autophagy, and glycolysis but promoted apoptosis in NSCLC cells

The endogenous level of circ_0005962 was knocked down to investigate the role of circ_0005962 in NSCLC cells. Si-circ_0005962 was inserted into the mature sequence of circ_0005962 to reduce circ_0005962 expression, with si-NC as a control (Figure 2a). Then, the knockdown efficiency was examined by qPCR, and the result showed that the expression of circ_0005962 in A549 and HCC827 cells with si-circ_0005962#1, si-circ_0005962#2, and si-circ_0005962#3 transfection was notably decreased compared to si-NC, and the knockdown efficiency in the si-circ_0005962#1 group was the highest (Figure 2b). Hence, si-circ_0005962#1 was chosen for the following analyses. The result of CCK-8 assay revealed that cell proliferation was prominently suppressed in A549 and HCC827 cells transfected with si-circ_0005962#1 (Figure 2c). On the contrary, flow cytometry assay presented that the apoptosis rate in A549 and HCC827 cells with si-circ_0005962#1 transfection was inversely enhanced (Figure 2d). Besides, the protein levels of autophagy-related markers were quantified to assess the change of autophagy, and we found that the levels of Beclin 1 and LC3-II/LC3-I were declined with circ_0005962 knockdown (Figure 2e and f). Moreover, the level of glucose in the culture medium and the production of lactate were checked to assess glycolysis progression, and we noticed that the level of existing glucose in A549 and HCC827 cells with si-circ_0005962#1 transfection was higher than that with si-NC transfection, suggesting that the consumptive glucose was reduced (Figure 2g). The level of lactate production was significantly blocked in A549 and HCC827 cells with si-circ_0005962#1 transfection relative to si-NC (Figure 2h). All data clarified that circ_0005962 knockdown inhibited proliferation, autophagy, and glycolysis but induced apoptosis in NSCLC cells.

3.3 miR-382-5p was a target of circ_0005962

To determine whether circ_0005962 functioned by acting as a ceRNA to modulate the expression of target miRNAs, the putative target miRNAs were predicted by the online tool circInteractome. The analysis showed that miR-382-5p was one of target miRNAs of circ_0005962 with specific binding sites (Figure 3a). To ascertain the relationship

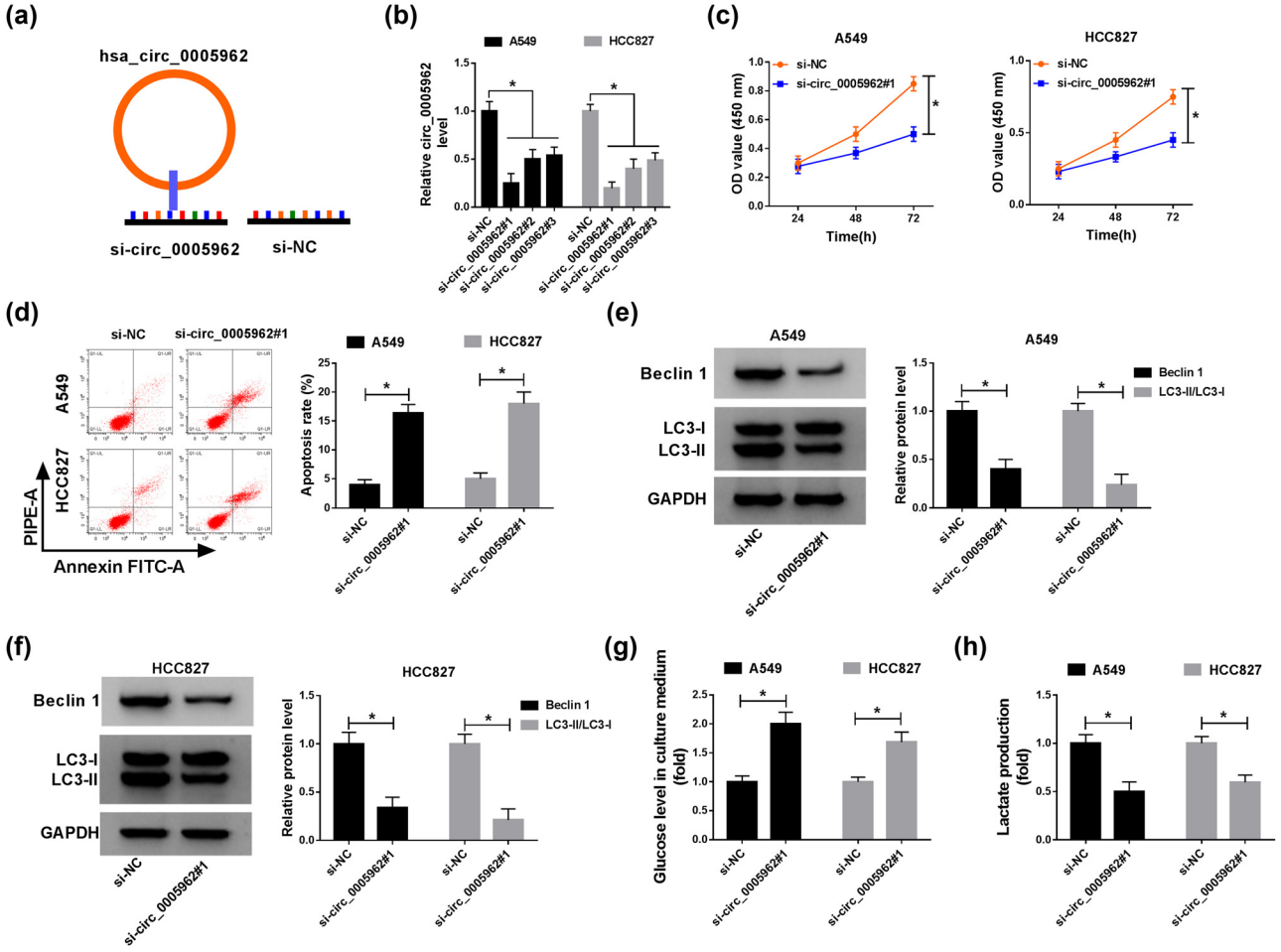

Figure 2: circ_0005962 knockdown inhibited proliferation, autophagy, and glycolysis but contributed to apoptosis in NSCLC cells. (a) The diagram of circ_0005962 knockdown. (b) The efficiency of circ_0005962 knockdown in different transfection lines was detected by qPCR. A549 and HCC827 cells were transfected with si-circ_0005962#1 or si-NC. (c) Cell proliferation was assessed by CCK-8 assay. (d) Cell apoptosis was executed by flow cytometry assay. (e and f) The protein levels of Beclin 1 and LC3-II/LC3-I were quantified by western blot. (g and h) The glycolysis progression was evaluated according to the level of glucose in culture medium and lactate production. $*P < 0.05$.

between circ_0005962 and miR-382-5p, dual-luciferase reporter assay and RIP assay were performed. The luciferase activity in A549 and HCC827 cells with circ_0005962-wt and miR-382-5p transfection was substantially decreased compared with circ_0005962-wt and NC transfection, while the luciferase activity in A549 and HCC827 cells with circ_0005962-mut and miR-382-5p transfection was unchanged compared with circ_0005962-mut and NC transfection (Figure 3b). RIP analysis presented that both circ_0005962 and miR-382-5p were significantly enriched in the Ago2 pellet of A549 and HCC827 lysate compared to IgG control (Figure 3c). Moreover, qPCR analysis exhibited that the expression of miR-382-5p was notably declined with circ_0005962 overexpression but improved with circ_0005962 knockdown in A549 and HCC827 cells (Figure 3d). Additionally, the expression of miR-382-5p in NSCLC tumor tissues ($n = 45$) was markedly weaker than that in normal tissues ($n = 45$) (Figure 3e). The expression of miR-382-5p was also lower in A549 and HCC827 cells than that in BEAS-2B cells (Figure 3f). Spearman's correlation coefficient revealed that circ_0005962 expression was negatively correlated with miR-382-5p expression in NSCLC tissues (Figure 3g). These analyses maintained that miR-382-5p was a target of circ_0005962, and its expression was suppressed by circ_0005962.

3.4 Inhibition of miR-382-5p reversed the role of circ_0005962 knockdown in NSCLC cells

A549 and HCC827 cells were introduced with si-circ_0005962#1, si-NC, si-circ_0005962#1 + anti-miR-382-5p and si-circ_0005962#1 + anti-NC, respectively. First, the expression of miR-382-5p in these transfected cells was checked,

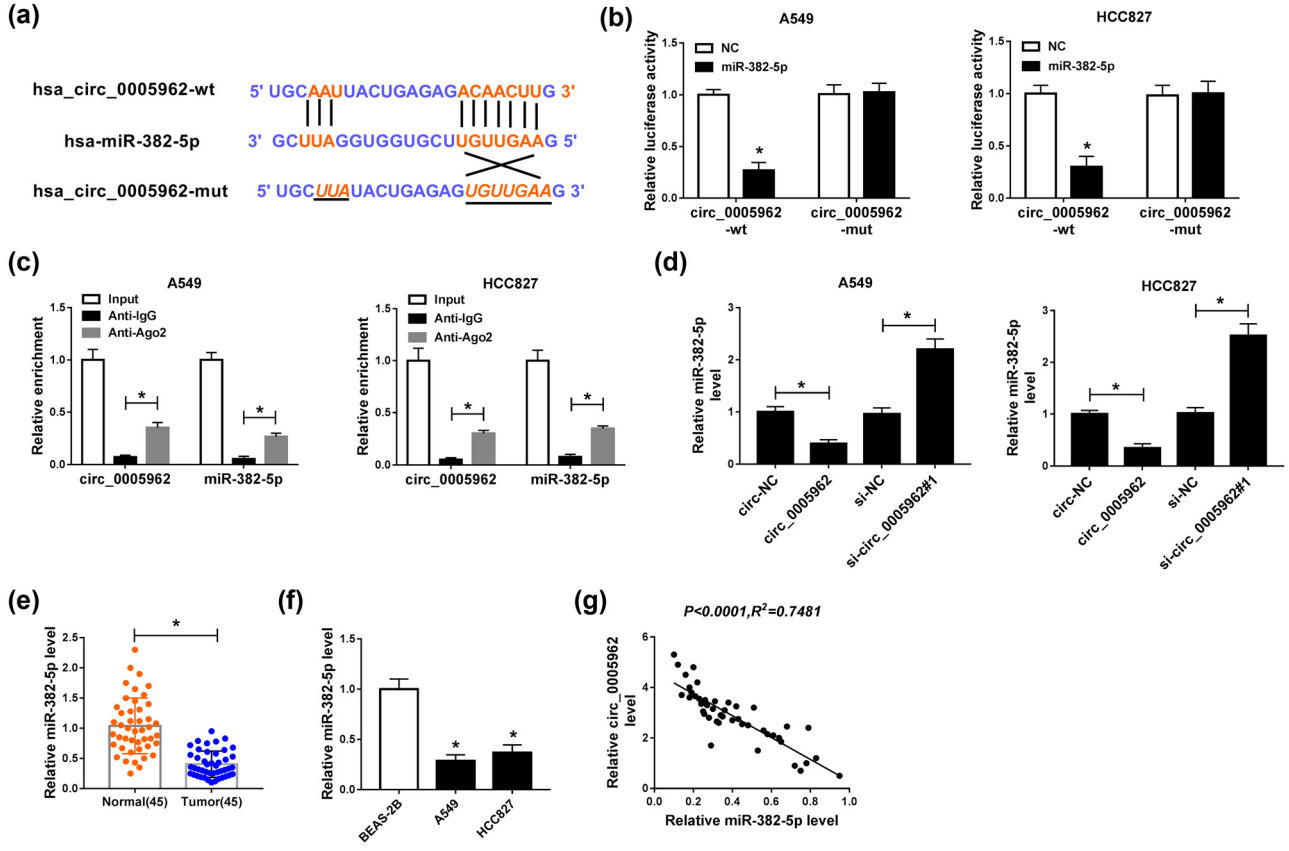

Figure 3: miR-382-5p was a target of circ_0005962. (a) The binding sites between circ_0005962 and miR-382-5p were analyzed by the online tool circInteractome. (b) The relationship between circ_0005962 and miR-382-5p was verified by dual-luciferase reporter assay. (c) The relationship between circ_0005962 and miR-382-5p was further confirmed by RIP assay. (d) The expression of miR-382-5p in A549 and HCC827 cells transfected with circ_0005962 or si-circ_0005962 was detected by qPCR. (e and f) The expression of miR-382-5p in NSCLC tissues and cell lines was detected by qPCR. (g) The correlation between circ_0005962 and miR-382-5p was analyzed by Spearman's correlation coefficient. *$P < 0.05$.

and we found that the expression of miR-382-5p was enhanced in the si-circ_0005962#1 group but inhibited in the si-circ_0005962#1 + anti-miR-382-5p group (Figure 4a). Cell proliferation inhibited by si-circ_0005962#1 transfection was recovered in A549 and HCC827 cells with si-circ_0005962#1 + anti-miR-382-5p transfection (Figure 4b). The elevated apoptosis rate of cells with si-circ_0005962#1 transfection was suppressed in cells with si-circ_0005962#1 + anti-miR-382-5p transfection (Figure 4c). The protein levels of Beclin 1 and LC3-II/LC3-I were depleted in A549 and HCC827 cells transfected with si-circ_0005962#1 but restored in cells transfected with si-circ_0005962#1 + anti-miR-382-5p (Figure 4d and e). The level of existing glucose in medium in the si-circ_0005962#1 + anti-miR-382-5p group was declined than that in the si-circ_0005962#1 group (Figure 4f). The level of lactate production inhibited in the si-circ_0005962#1 group was largely promoted in the si-circ_0005962#1 + anti-miR-382-5p group (Figure 4g). These results indicated that circ_0005962 knockdown inhibited proliferation, autophagy, and glycolysis but induced apoptosis by enhancing the expression of miR-382-5p.

3.5 PDK4 was a target of miR-382-5p

The circRNA–miRNA–mRNA regulatory network is an important mechanism in the development of human cancers. The target mRNAs of miR-382-5p were analyzed to observe whether circ_0005962 played functions following this mechanism. Online bioinformatics tool starbase predicted that PDK4 was one of the targets of miR-382-5p with a specific binding site at its 3′UTR (Figure 5a). Besides, miR-382-5p overexpression predominantly inhibited the luciferase activity in A549 and HCC827 cells transfected with PDK4-wt but not PDK4-mut (Figure 5b). Moreover, the enrichment of PDK4 was notably elevated in the miR-382-5p-transfected group compared with that in the NC group after Ago2 RIP, while enrichment of PDK4 after IgG

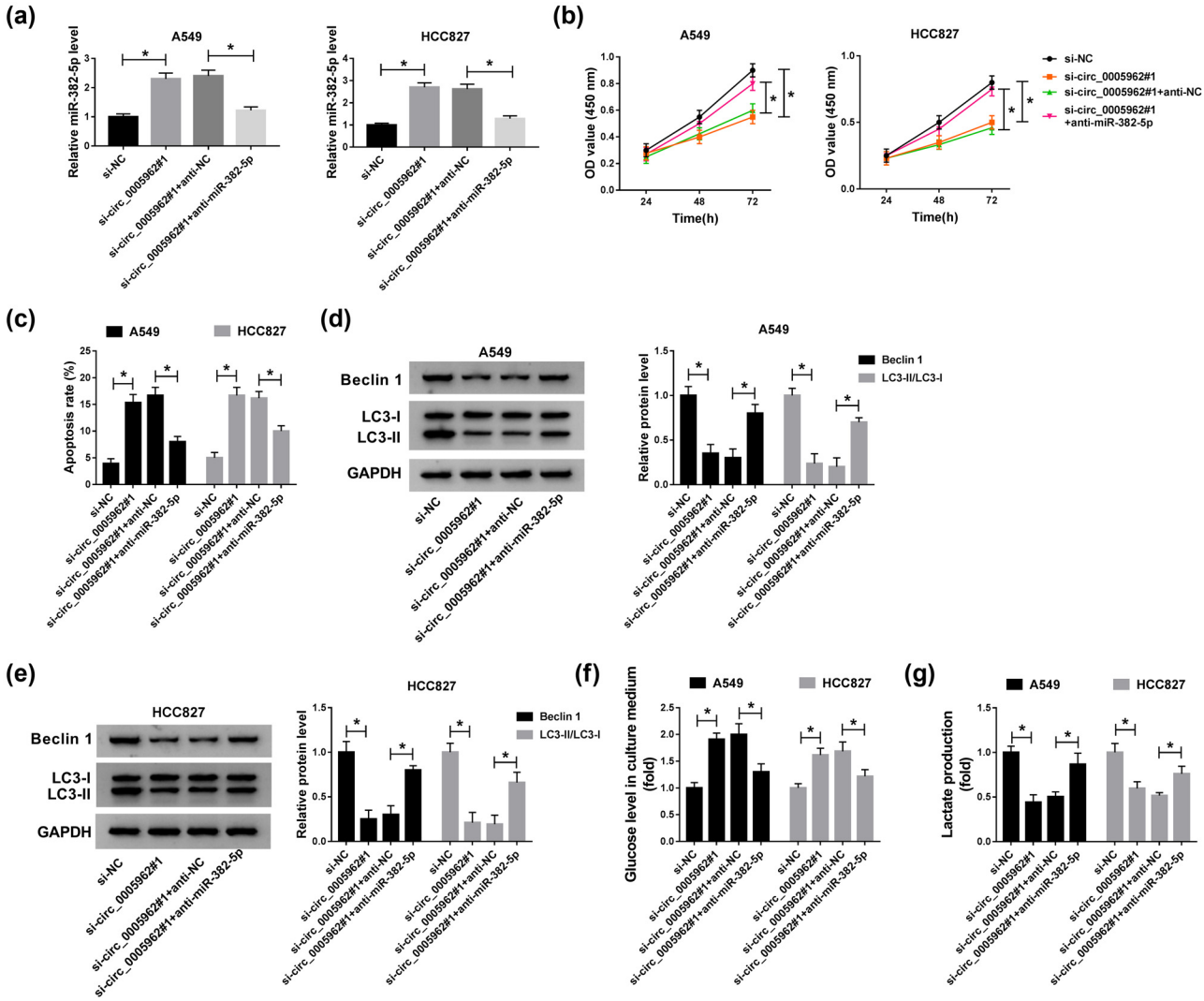

Figure 4: Inhibition of miR-382-5p reversed the role of circ_0005962 knockdown. A549 and HCC827 cells were introduced with si-circ_0005962#1, si-NC, si-circ_0005962#1 + anti-miR-382-5p or si-circ_0005962#1 + anti-NC. (a) The transfection efficiency was examined by qPCR. (b) Cell proliferation was assessed by CCK-8 assay. (c) Cell apoptosis was executed by flow cytometry assay. (d and e) The protein levels of Beclin 1 and LC3-II/LC3-I were quantified by western blot. (f and g) The glycolysis progression was evaluated according to the levels of glucose in culture medium and lactate production. *$P < 0.05$.

RIP showed no efficacy (Figure 5c). Next, western blot analysis monitored that the level of PDK4 was weakened in A549 and HCC827 cells with miR-382-5p transfection but elevated in cells with circ_0005962 + miR-382-5p transfection (Figure 5d). Also, the expression of PDK4 was detected in NSCLC tumor tissues, and the result presented that the expression of PDK4 at both mRNA and protein levels was abnormally higher in NSCLC tumor tissues ($n = 45$) relative to normal tissues ($n = 45$) (Figure 5e and f). Likewise, the protein level of PDK4 in A549 and HCC827 cells was also enhanced compared to BEAS-2B cells (Figure 5g). Furthermore, the mRNA level of PDK4 was positively correlated with circ_0005962 level but negatively correlated with the miR-382-5p level in NSCLC tissues (Figure 5h and i). All data suggested that PDK4 was a target of miR-382-5p, and circ_0005962 regulated the expression of PDK4 by targeting miR-382-5p.

3.6 PDK4 overexpression abolished the role of miR-382-5p reintroduction in NSCLC cells

A549 and HCC827 cells were introduced with miR-382-5p, NC, miR-382-5p + PDK4 and miR-382-5p + vector,

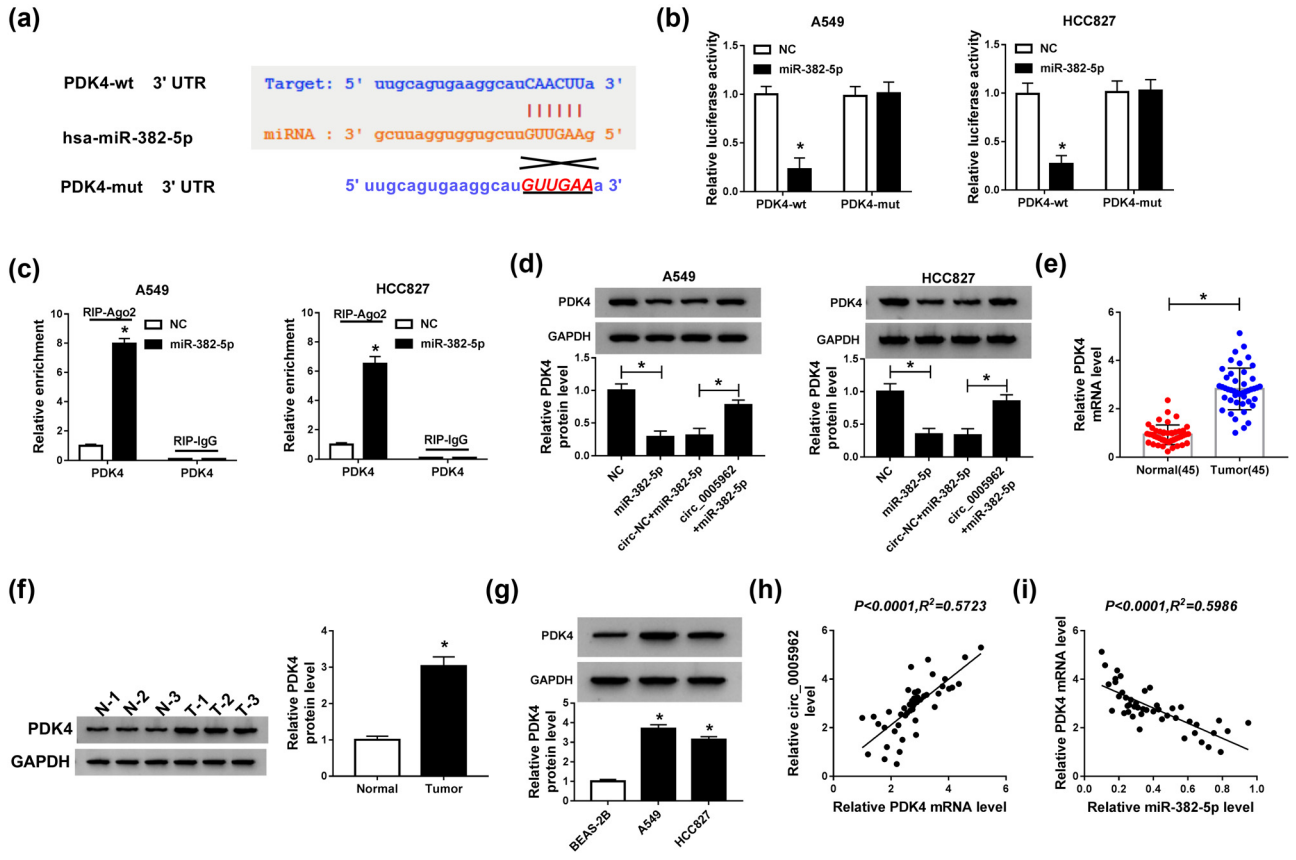

Figure 5: PDK4 was a target of miR-382-5p. (a) The binding sites between PDK4 3′UTR and miR-382-5p were analyzed by online tool starbase. (b) The relationship between PDK4 and miR-382-5p was verified by dual-luciferase reporter assay. (c) The relationship between PDK4 and miR-382-5p was further confirmed by RIP assay. (d) The expression of PDK4 at the protein level in A549 and HCC827 cells transfected with miR-382-5p or circ_0005962 + miR-382-5p was detected by western blot. (e and f) The expression of PDK4 at mRNA and protein levels in NSCLC tissues was detected by qPCR and western blot. (g) The protein level of PDK4 in NSCLC cell lines was detected by western blot. (h and i) The correlation between PDK4 and circ_0005962 or miR-382-5p was analyzed by Spearman's correlation coefficient. *$P < 0.05$.

respectively. The expression of PDK4 was examined to assess transfection efficiency, and the result showed that the level of PDK4 was obviously reduced in cells transfected with miR-382-5p but regained in cells transfected with miR-382-5p + PDK4 (Figure 6a). In function, cell proliferation was inhibited by the reintroduction of miR-382-5p but promoted by the combination of miR-382-5p reintroduction and PDK4 overexpression (Figure 6b). The apoptosis rate was elevated by miR-382-5p reintroduction but restrained by the combination of miR-382-5p reintroduction and PDK4 overexpression (Figure 6c). Moreover, the levels of Beclin1 and LC3-II/LC3-I were weakened in A549 and HCC827 cells transfected with miR-382-5p but rescued in cells transfected with miR-382-5p + PDK4 (Figure 6d and e). The existing glucose level was abundant in the miR-382-5p group but reduced in the miR-382-5p + PDK4 group, suggesting that PDK4 overexpression enhanced the level of glucose consumption inhibited by miR-382-5p reintroduction (Figure 6f). The level of lactate production was blocked by miR-382-5p reintroduction but recovered by the combination of miR-382-5p reintroduction and PDK4 overexpression (Figure 6g). These data hinted that miR-382-5p attenuated cell proliferation, autophagy, and glycolysis but contributed to apoptosis by inhibiting the expression of PDK4.

3.7 circ_0005962 knockdown inhibited tumor growth *in vivo*

A549 cells with stable Lv-sh-circ_0005962 transfection were subcutaneously injected into the groin of nude mice to determine the role of circ_0005962 *in vivo*. As shown in Figure 7a and b, circ_0005962 knockdown remarkably reduced tumor volume and tumor weight. After injection for 5 weeks, all mice were killed, and the

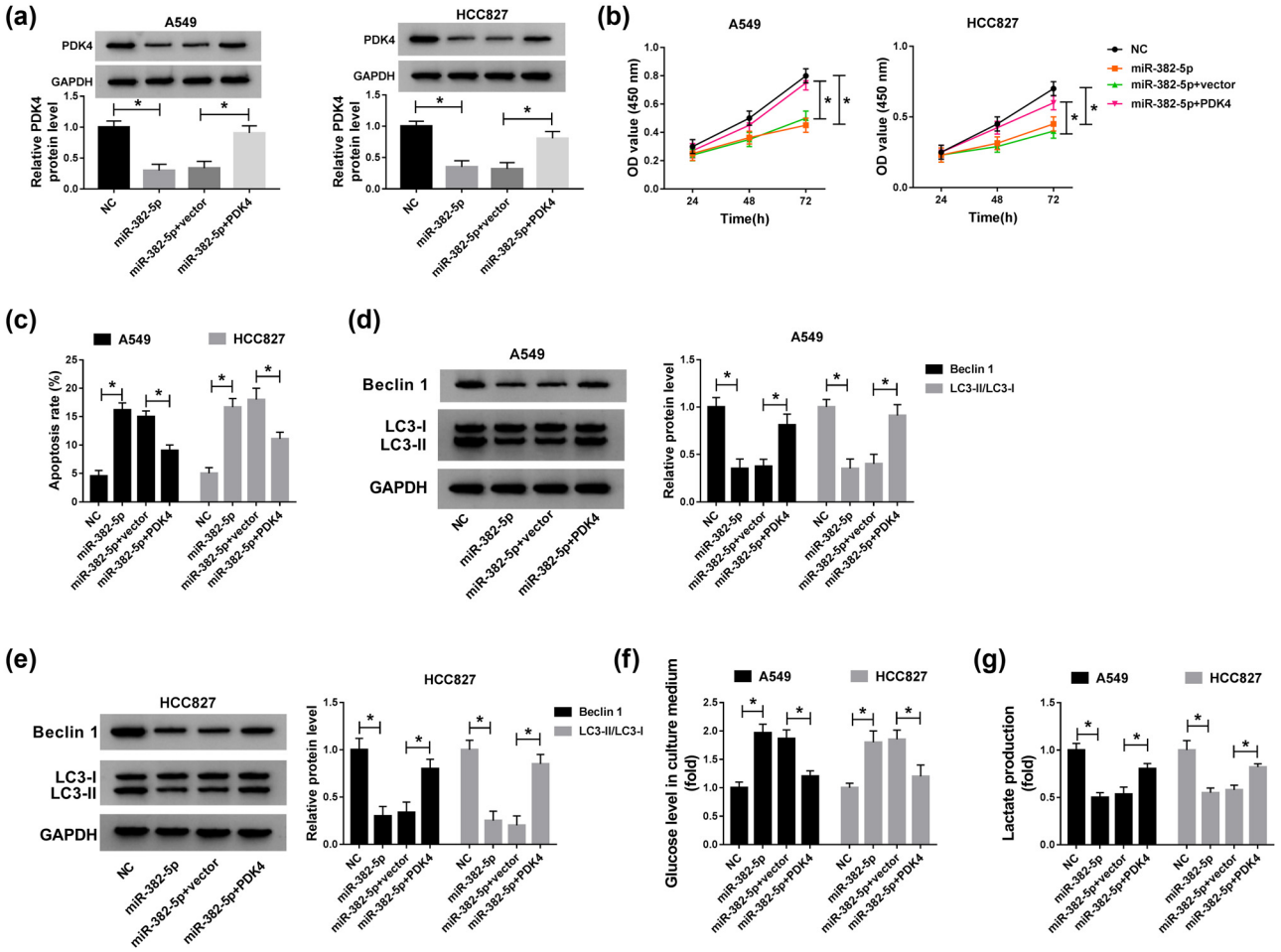

Figure 6: PDK4 overexpression abrogated the role of miR-382-5p reintroduction. A549 and HCC827 cells were transfected with miR-382-5p, NC, miR-382-5p + PDK4, or miR-382-5p + vector. (a) The transfection efficiency was checked according to the expression level of PDK4 using western blot. (b) Cell proliferation was assessed by CCK-8 assay. (c) Cell apoptosis was monitored by flow cytometry assay. (d and e) The protein levels of Beclin 1 and LC3-II/LC3-I were quantified by western blot. (f and g) The glycolysis progression was evaluated according to the level of glucose in culture medium and lactate production. *$P < 0.05$.

tumors were removed for expression analysis. The expression of circ_0005962 and PDK4 mRNA were noticeably declined in the Lv-sh-circ_0005962 group, while the expression of miR-382-5p was conspicuously strengthened in the Lv-sh-circ_0005962 group (Figure 7c). Besides, the protein level of PDK4 was consistent with its mRNA level. Additionally, the levels of apoptosis-related marker (C-caspase 3), proliferation-related marker (PCNA), and autophagy-related markers (Beclin 1 and LC3-II/LC3-I) were monitored, and we discovered that the level of C-caspase 3 was notably reinforced, while the levels of PCNA, Beclin 1, and LC3-II/LC3-I were notably impaired in the Lv-sh-circ_0005962 group (Figure 7d). Collectively, circ_0005962 knockdown impeded tumor growth *in vivo*.

4 Discussion

NSCLC is a severe burden to people's lives, and the prognosis of NSCLC patients is still unsatisfactory. The responses to existing standard therapies are poor, except for the most localized cancers [26]. Hence, more novel mechanisms of NSCLC progression need to be explored to develop aimed therapeutic strategies for NSCLC. Here, we investigated the role of circ_0005962 in NSCLC for the first time. circ_0005962 was observed to be aberrantly overexpressed in NSCLC tissues and cells. Functional analysis concluded that circ_0005962 knockdown blocked NSCLC progression *in vitro* and *in vivo*. Stepwise identification manifested that circ_0005962 could directly bind to miR-382-5p, leading to

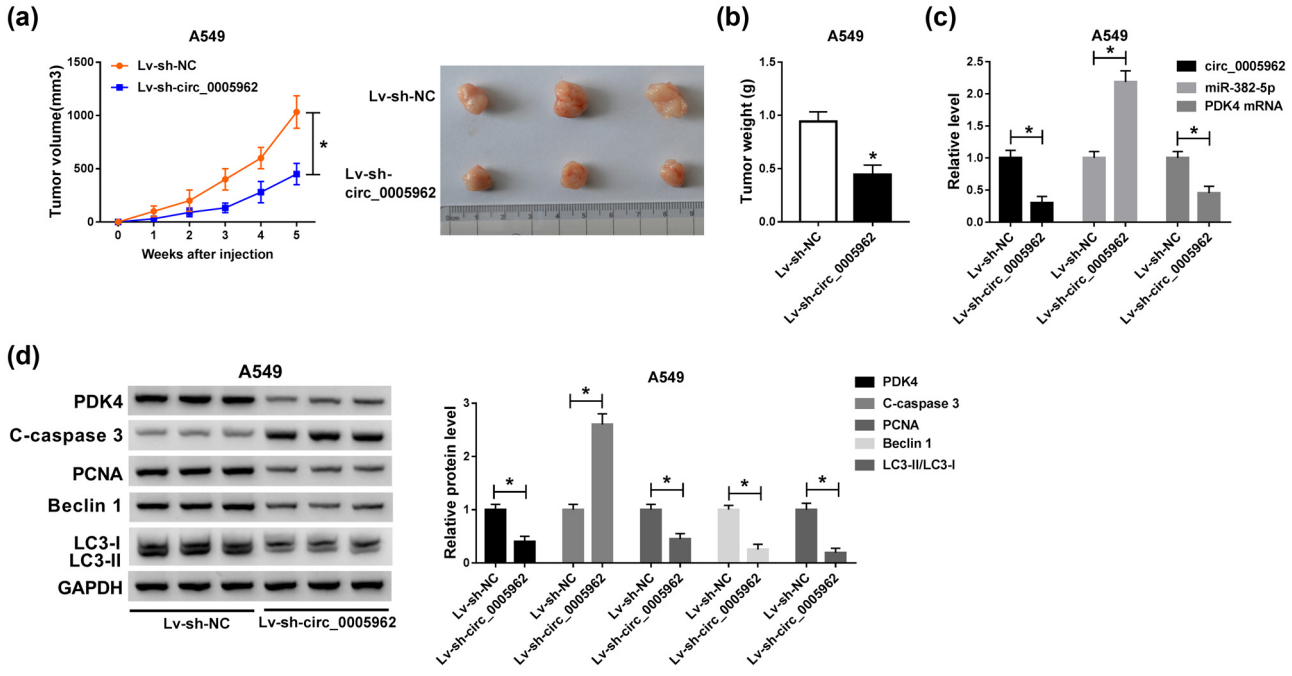

Figure 7: circ_0005962 knockdown depleted tumor growth *in vivo*. (a) The tumor volume was recorded once a week, lasting 5 weeks. (b) The tumor weight was measured after 5 weeks. (c) The expression of circ_0005962, miR-382-5p, and PDK was examined in excised tumor tissues by qPCR. (d) The protein levels of PDK4, C-caspase 3, and PCNA were quantified by western blot. *$P < 0.05$.

an increase of PDK4 expression, thereby contributing to the development of NSCLC. Our study illustrated the importance and carcinogenesis of circ_0005962 in NSCLC.

circRNAs were documented to be dysregulated in numerous human cancers, their dysfunction took effects on apoptosis, autophagy, chemoresistance, metastasis, and glycolysis [27–30]. Up to now, dozens of NSCLC-related circRNAs were screened and identified, such as circ_100146, circ-PRMT5, and circ_0026134 [11,31], leading to the malignant progression of NSCLC via acting as oncogenes. On the contrary, certain circRNAs, such as circPTPRA, circ_0001946, and circSMARCA5 were maintained as tumor suppressors to block NSCLC deterioration [28,32,33]. These data suggested the diverse roles of circRNAs in cancer development. Despite the fact that the role of several circRNAs was partly characterized, numerous circRNAs were lacking functional exploration. A previous study predicted differentially expressed circRNAs in lung adenocarcinoma using Gene Expression Omnibus (GEO) dataset and found that circ_0005962 was highly expressed in lung adenocarcinoma plasma and cells [14]. In view of this finding, we speculated that dysregulation of circ_0005962 might be associated with the malignant progression of NSCLC. Interestingly, we discovered that circ_0005962 knockdown inhibited cell proliferation, autophagy, and glycolysis but accelerated cell apoptosis *in vitro*. The aggressive growth of cancer cells was satisfied by the enhanced glycolysis metabolism, and the inhibition of glycolysis was served as a strategy for cancer treatment [34]. Autophagy contributes to nutrient recycling and metabolic adaptation and plays a dichotomous role in cancer development, inhibiting tumor inhibition or promoting tumor progression [35]. Accumulating evidence suggests that autophagy inhibition is a promising approach for the treatment of advanced cancer [36]. Our findings showed that glycolysis and autophagy were blocked by circ_0005962 knockdown, strongly suggesting that circ_0005962 might function as an oncogene at least in NSCLC progression.

In our study, miR-382-5p was identified as a target of circ_0005962. The role of miR-382 in NSCLC was gradually clear to function as a tumor suppressor. For example, miR-382 suppressed proliferation and migration of NSCLC cells by binding to the 3′UTR of LMO3 [37]. Besides, miR-382 was significantly downregulated in NSCLC tissues and cells, and enrichment of miR-382 depleted cell proliferation, migration, and invasion through targeting SETD8 [38]. Consistent with these findings, we also detected that miR-382-5p was weakly expressed in NSCLC cells, and reintroduction of miR-382-5p inhibited proliferation, autophagy, and glycolysis of NSCLC cells. Besides, miR-382-5p inhibition reversed the regulatory effects of circ_0005962 knockdown.

Considering the habitual action mode of miRNAs, we further analyzed the potential target mRNAs of miR-382-5p

to establish a detailed action mechanism of circ_0005962 in NSCLC. Among the mRNAs whose levels were increased in A549 and HCC827 cells, the increase of PDK4 expression was the most significant. Similarly, PDK4 has been reported to be highly expressed in cisplatin-resistant lung adenocarcinoma [39]. Besides, oncogene LINC00243 contributed to proliferation and glycolysis in NSCLC by positively regulating PDK4 [23]. Consistently, we also noticed that PDK4 overexpression eliminated the role of miR-382-5p reintroduction, leading to the malignant activities of NSCLC cells. These data indicated that PDK4 played a carcinogenic role in NSCLC.

Taken together, the expression of circ_0005962 was increased in NSCLC tissues and cell lines. Knockdown of LINC00243 blocked cell proliferation, autophagy, and glycolysis but accelerated cell apoptosis *in vitro* and weakened tumor growth *in vivo*. Moreover, circ_0005962 played these functions in NSCLC progression by activating the expression of PDK4 via sponging miR-382-5p. Our results not only corroborate the role of circ_0005962 in NSCLC but also provide the circ_0005962/miR-382-5p/PDK4 regulatory axis, which may be promising to develop novel therapeutic approaches for NSCLC.

Funding information: This work was supported by study on the sensitization effect of EGFR inhibitors on radiotherapy combined with PD-L1 inhibitor to stimulate the remote effect (WJ2019H173).

Conflict of interest: The authors declare that they have no conflicts of interest.

Data availability statement: The datasets generated during and/or analysed during the current study are available from the corresponding author on reasonable request.

References

[1] Magnuson WJ, Yeung JT, Guillod PD, Gettinger SN, Yu JB, Chiang VL. Impact of deferring radiation therapy in patients with epidermal growth factor receptor-mutant non-small cell lung cancer who develop brain metastases. Int J Radiat Oncol Biol Phys. 2016;95:673–9.

[2] Testa U, Castelli G, Pelosi E. Lung cancers: molecular characterization, clonal heterogeneity and evolution, and cancer stem cells. Cancers (Basel). 2018;10:248.

[3] Zhukovsky M, Varaksin A, Pakholkina O. Statistical analysis of observational study of the influence of radon and other risk factors on lung cancer incidence. Radiat Prot Dosimetry. 2014;160:108–11.

[4] Barnett SA, Downey RJ, Zheng J, Plourde G, Shen R, Chaft J, et al. Utility of routine PET imaging to predict response and survival after induction therapy for non-small cell lung cancer. Ann Thorac Surg. 2016;101:1052–9.

[5] Brody H. Lung cancer. Nature. 2014;513:S1.

[6] Laskin JJ, Sandler AB. State of the art in therapy for non-small cell lung cancer. Cancer Invest. 2005;23:427–42.

[7] Salzman J, Gawad C, Wang PL, Lacayo N, Brown PO. Circular RNAs are the predominant transcript isoform from hundreds of human genes in diverse cell types. PLoS One. 2012;7:e30733.

[8] Hansen TB, Jensen TI, Clausen BH, Bramsen JB, Finsen B, Damgaard CK, et al. Natural RNA circles function as efficient microRNA sponges. Nature. 2013;495:384–8.

[9] Kulcheski FR, Christoff AP, Margis R. Circular RNAs are miRNA sponges and can be used as a new class of biomarker. J Biotechnol. 2016;238:42–51.

[10] Liang D, Wilusz JE. Short intronic repeat sequences facilitate circular RNA production. Genes Dev. 2014;28:2233–47.

[11] Chen L, Nan A, Zhang N, Jia Y, Li X, Ling Y, et al. Circular RNA 100146 functions as an oncogene through direct binding to miR-361-3p and miR-615-5p in non-small cell lung cancer. Mol Cancer. 2019;18:13.

[12] Wang T, Wang X, Du Q, Wu N, Liu X, Chen Y, et al. The circRNA circP4HB promotes NSCLC aggressiveness and metastasis by sponging miR-133a-5p. Biochem Biophys Res Commun. 2019;513:904–11.

[13] Tan S, Sun D, Pu W, Gou Q, Guo C, Gong Y, et al. Circular RNA F-circEA-2a derived from EML4-ALK fusion gene promotes cell migration and invasion in non-small cell lung cancer. Mol Cancer. 2018;17:138.

[14] Liu XX, Yang YE, Liu X, Zhang MY, Li R, Yin YH, et al. A two-circular RNA signature as a noninvasive diagnostic biomarker for lung adenocarcinoma. J Transl Med. 2019;17:50.

[15] Jiang C, Hu X, Alattar M, Zhao H. miRNA expression profiles associated with diagnosis and prognosis in lung cancer. Expert Rev Anticancer Ther. 2014;14:453–61.

[16] Wang J, Chen C, Yan X, Wang P. The role of miR-382-5p in glioma cell proliferation, migration and invasion. Onco Targets Ther. 2019;12:4993–5002.

[17] Sun LP, Xu K, Cui J, Yuan DY, Zou B, Li J, et al. Cancerassociated fibroblastderived exosomal miR3825p promotes the migration and invasion of oral squamous cell carcinoma. Oncol Rep. 2019;42:1319–28.

[18] Ho JY, Hsu RJ, Liu JM, Chen SC, Liao GS, Gao HW, et al. microRNA-382-5p aggravates breast cancer progression by regulating the RERG/Ras/ERK signaling axis. Oncotarget. 2017;8:22443–59.

[19] Jeoung NH. Pyruvate dehydrogenase kinases: therapeutic targets for diabetes and cancers. Diabetes Metab J. 2015;39:188–97.

[20] Vander Heiden MG, Cantley LC, Thompson CB. Understanding the Warburg effect: the metabolic requirements of cell proliferation. Science. 2009;324:1029–33.

[21] Wang J, Qian Y, Gao M. Overexpression of PDK4 is associated with cell proliferation, drug resistance and poor prognosis in ovarian cancer. Cancer Manag Res. 2019;11:251–62.

[22] Yang R, Zhu Y, Wang Y, Ma W, Han X, Wang X, et al. HIF-1alpha/PDK4/autophagy pathway protects against advanced

glycation end-products induced vascular smooth muscle cell calcification. Biochem Biophys Res Commun. 2019;517:470–6.
[23] Feng X, Yang S. Long non-coding RNA LINC00243 promotes proliferation and glycolysis in non-small cell lung cancer cells by positively regulating PDK4 through sponging miR-507. Mol Cell Biochem. 2019;463:127–36.
[24] Wang Y, Zhang J, Li J, Gui R, Nie X, Huang R. circRNA_014511 affects the radiosensitivity of bone marrow mesenchymal stem cells by binding to miR-29b-2-5p. Bosn J Basic Med Sci. 2019;19:155–63.
[25] Ren W, Wu S, Wu Y, Liu T, Zhao X, Li Y. microRNA-196a/-196b regulate the progression of hepatocellular carcinoma through modulating the JAK/STAT pathway via targeting SOCS2. Cell Death Dis. 2019;10:333.
[26] Lemjabbar-Alaoui H, Hassan OU, Yang YW, Buchanan P. Lung cancer: Biology and treatment options. Biochim Biophys Acta. 2015;1856:189–210.
[27] Chi G, Xu D, Zhang B, Yang F. Matrine induces apoptosis and autophagy of glioma cell line U251 by regulation of circRNA-104075/BCL-9. Chem Biol Interact. 2019;308:198–205.
[28] Wei S, Zheng Y, Jiang Y, Li X, Geng J, Shen Y, et al. The circRNA circPTPRA suppresses epithelial-mesenchymal transitioning and metastasis of NSCLC cells by sponging miR-96-5p. EBioMedicine. 2019;44:182–93.
[29] Kun-Peng Z, Xiao-Long M, Lei Z, Chun-Lin Z, Jian-Ping H, Tai-Cheng Z. Screening circular RNA related to chemotherapeutic resistance in osteosarcoma by RNA sequencing. Epigenomics. 2018;10:1327–46.
[30] Ren S, Liu J, Feng Y, Li Z, He L, Li L, et al. Knockdown of circDENND4C inhibits glycolysis, migration and invasion by up-regulating miR-200b/c in breast cancer under hypoxia. J Exp Clin Cancer Res. 2019;38:388.
[31] Chang H, Qu J, Wang J, Liang X, Sun W. Circular RNA circ_0026134 regulates non-small cell lung cancer cell proliferation and invasion via sponging miR-1256 and miR-1287. Biomed Pharmacother. 2019;112:108743.
[32] Wang Y, Li H, Lu H, Qin Y. Circular RNA SMARCA5 inhibits the proliferation, migration, and invasion of non-small cell lung cancer by miR-19b-3p/HOXA9 axis. Onco Targets Ther. 2019;12:7055–65.
[33] Huang MS, Liu JY, Xia XB, Liu YZ, Li X, Yin JY, et al. Hsa_circ_0001946 inhibits lung cancer progression and mediates cisplatin sensitivity in non-small cell lung cancer via the nucleotide excision repair signaling pathway. Front Oncol. 2019;9:508.
[34] Akins NS, Nielson TC, Le HV. Inhibition of glycolysis and glutaminolysis: an emerging drug discovery approach to combat cancer. Curr Top Med Chem. 2018;18:494–504.
[35] Amaravadi RK, Kimmelman AC, Debnath J. Targeting autophagy in cancer: recent advances and future directions. Cancer Discov. 2019;9:1167–81.
[36] Onorati AV, Dyczynski M, Ojha R, Amaravadi RK. Targeting autophagy in cancer. Cancer. 2018;124:3307–18.
[37] Chen D, Zhang Y, Lin Y, Shen F, Zhang Z, Zhou J. microRNA-382 inhibits cancer cell growth and metastasis in NSCLC via targeting LMO3. Exp Ther Med. 2019;17:2417–24.
[38] Chen T, Ren H, Thakur A, Yang T, Li Y, Zhang S, et al. miR-382 inhibits tumor progression by targeting SETD8 in non-small cell lung cancer. Biomed Pharmacother. 2017;86:248–53.
[39] Yu S, Ren H, Li Y, Liang X, Ning Q, Chen X, et al. HOXA4-dependent transcriptional activation of AXL promotes cisplatin- resistance in lung adenocarcinoma cells. Anticancer Agents Med Chem. 2018;18:2062–7.